

Suppression of superconductivity in FeSe films under tensile strain

Y. F. Nie, E. Brahim, J. I. Budnick, W. A. Hines, M. Jain, and B. O. Wells

Department of Physics, University of Connecticut, Storrs, CT 06269

(Dated: November 14, 2018)

We have studied the effect of tensile strain on the superconductivity in FeSe films. 50 nm, 100 nm, and 200 nm FeSe films were grown on MgO, SrTiO₃, and LaAlO₃ substrates by using a pulsed laser deposition technique. X-ray diffraction analysis showed that the tetragonal phase is dominant in all of our FeSe films. The 50 nm FeSe films on MgO and SrTiO₃ are under tensile strain, while the 50 nm FeSe film on LaAlO₃ and the other thick FeSe films are unstrained. Superconducting transitions have been observed in unstrained FeSe films with $T_{onset} \approx 8$ K, which is close to the bulk value. However, no sign of superconductivity has been observed in FeSe films under tensile strain down to 5 K. This is evidence to show that tensile strain suppresses superconductivity in FeSe films.

PACS numbers: 74.78.Bz, 74.62.Bf, 74.62.Fj

Since the discovery of superconductivity in doped LaOFeAs with a T_c of 26 K by Kamihara et al. [1], the pnictide superconductors have attracted much attention [2, 3, 4]. Just as the CuO₂ plane plays a key role in high T_c superconducting copper oxides [5], the FeAs layer is believed to be crucial to the superconductivity in iron-arsenide [4]. Stimulated by this discovery, other iron-based planar compounds have been investigated in a search for superconductivity [6, 7, 8].

Recently, superconductivity was observed in α -FeSe with a transition temperature $T_c \approx 8$ K [8]. α -FeSe with the tetragonal PbO structure has an Fe-based planar sublattice equivalent to the layered iron-based quaternary oxypnictides. Thus, it is expected that the study of superconductivity in FeSe will be valuable in understanding the superconducting mechanism of pnictide superconductors. FeSe has a complicated phase diagram [9, 10]. The superconductivity of FeSe can be enhanced by partially replacing Se with Te, where T_c reaches a maximum of 15.2 K at about 50% Te substitution [11]. Also, it has been reported that the T_c of α -FeSe has a strong dependence on hydrostatic pressure, and can be enhanced up to 27 K by applying a pressure of 1.48 GPa [12]. Another study reported that the application of hydrostatic pressure first rapidly increases T_c to a broad maximum of 37 K at 7 GPa, before decreasing to 6 K at 14 GPa [13]. A phase transition from tetragonal to orthorhombic has been reported at 12 GPa, with the high pressure orthorhombic phase having a higher T_c , reaching 34 K at 22 GPa [14]. There are additional studies of the pressure effects for FeSe bulk materials [15]. All of the studies imply that strain (compression) is a very important parameter for iron-based superconductivity.

In all of these high-pressure studies, the materials are under compression; however, how FeSe will behave under tension is still unknown. It is very important to study the tensile strain effect in order to understand the mechanism of iron-based superconductivity. It is difficult to introduce large tensile strain in a bulk material. On the contrary, it is relatively easy to introduce large strain in epitaxial films, both compressive and tensile. Strain in

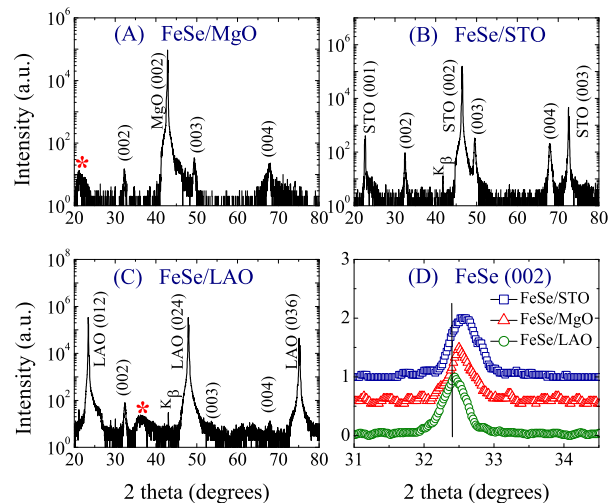


FIG. 1: (color online) X-ray diffraction profiles for 50 nm FeSe films on MgO, STO, and LAO substrates at room temperature. The panel (D) illustrates the effect of in-plane strain on the FeSe (002) peaks, with peaks normalized to an intensity of one and offset for clarity.

films differs from the hydrostatic pressure in bulk in that film strain is biaxial. However, for a layered material, biaxial strain may be the most interesting. The biaxial strain comes from the energetically beneficial registry growth of the films on selected substrates. Coherently strained films in which the film and substrate in-plane lattice parameters are forced to match can be maintained up to a critical thickness, which is of the order of a few nanometers, depending on the amount of the mismatch. Above the critical thickness, the strain energy becomes so large that it is then energetically favorable to nucleate misfit dislocations [16]. By properly choosing the substrate and film thickness, we can grow films with various tensile strains. In this report, we present a study of the tensile strain effect on the superconductivity in FeSe films.

The FeSe films studied were grown on (001) MgO,

(001) SrTiO₃ (STO), and (001) LaAlO₃ (LAO) single crystal substrates. The calculated lattice mismatch values, defined as the percentage difference between bulk FeSe and substrate in-plane lattice parameters, are listed in Table I. The MgO substrate gives the largest lattice mismatch, while the LAO substrate nearly matches the lattice constants of bulk FeSe. The STO substrate has an intermediate lattice mismatch. We studied 50 nm FeSe films on all substrates, 100 nm on STO, and 200 nm on MgO and LAO. All films were grown by using a pulsed laser deposition (PLD) technique. The substrate temperature was kept at 380 °C in 10⁻⁶ torr vacuum during the deposition. After the deposition, the samples were slowly cooled down to room temperature in vacuum. The growth parameters were studied carefully in order to get the best epitaxial growth of tetragonal α -FeSe films. The growth temperature is found to be the most critical parameter. At high temperature (\approx 800 °C), no film was grown on the substrate. At a temperature between 450 °C and 800 °C, FeSe films tend to grow hexagonal and other extra phases. Only those films grown at lower temperature (\approx 380 °C) have the best tetragonal phase along with good mosaics.

A two-circle x-ray diffractometer (XRD) with monochromatic CuK α ($\lambda=1.540598$ Å) radiation was used to determine the lattice constants of the FeSe films. The film resistance was measured by using the 4-point technique. Temperatures (5 K \leq T \leq 300 K) and magnetic fields (0 \leq H \leq 9 T) were obtained using the Quantum Design PPMS system.

TABLE I: Out-of-plane lattice constants (c) for FeSe films.

Substrate ^a	Lattice Mismatch	Film Thickness	c -value
STO	3.7 %	50 nm	5.49 Å
MgO	12 %	50 nm	5.50 Å
LAO	0.64 %	50 nm	5.52 Å
STO	3.7 %	100 nm	5.51 Å
MgO	12 %	200 nm	5.52 Å
LAO	0.64 %	200 nm	5.51 Å

^aBulk FeSe is tetragonal ($a=b=3.765$ Å, $c=5.518$ Å); STO is cubic ($a=3.905$ Å), MgO is cubic ($a=4.216$ Å); and LAO is rhombohedral ($a=3.789$ Å, $c=13.11$ Å).

The XRD patterns for the three 50 nm films are shown in Fig.1 using log scales. Panel (D) in Fig. 1 shows in detail the shift of the (002) peak due to the effect of in-plane strain on the out-of-plane lattice constant. The XRD patterns for the 100 nm and 200 nm FeSe films are similar to those shown in Fig. 1 with relatively stronger peaks. All of the tetragonal peaks were indexed using the P4/nmm space group. The FeSe films on STO show a pure tetragonal phase. No obvious hexagonal FeSe (NiAs-type) were observed for all these films. The extra peaks, which are due to second phases and the substrate's background, are marked by stars (*). The sharp small extra peaks are substrate K β peaks. The extra small

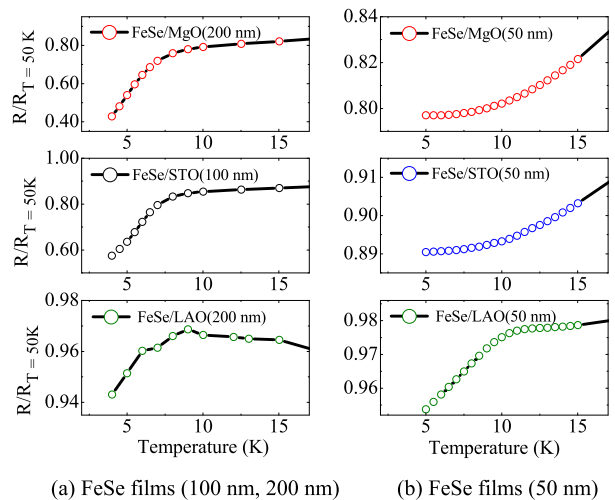


FIG. 2: (color online) Resistance as a function of temperature for: a) 100 nm and 200 nm and b) 50 nm FeSe films on MgO, STO, and LAO substrates.

broad background for the films on LAO probably results from imperfections of the LAO substrate. Overall, these results imply that the α -FeSe phase is dominant.

Out-of-plane lattice constants were calculated from the XRD data using the (002) peaks (see Fig. 1), and are listed in Table I. In our work, the FeSe films were found to be extremely sensitive to the storage atmosphere. When exposed to air for a short period of time (\approx hours), we observed the disappearance of the superconducting transition. This is possibly due to oxidation or other chemical reactions of the FeSe films. Epitaxial growth of the FeSe film was checked by using a four-circle diffractometer (GADDS). By comparing the out-of-plane lattice constants, we have calculated the in-plane strain. It is reasonable to assume that the smaller the out-of-plane lattice constants, the more tensile strain in the plane.

The out-of-plane lattice constants show that the FeSe films have the orientation with (001) normal to the substrate surface. The c -values for the 100 nm FeSe film on STO, 200 nm FeSe film on MgO and LAO are 5.51 Å, 5.52 Å, and 5.51 Å, respectively. We consider FeSe films with $c = 5.51$ Å and $c = 5.52$ Å as unstrained since our best estimate of the combined systematic and random error in the lattice constant to be about ± 0.01 Å. Compared to the bulk value of FeSe ($c = 5.518$ Å), the three thicker FeSe films are unstrained. This is because the 100 nm and 200 nm thicknesses are above the relaxation critical thickness. The 50 nm FeSe film on LAO are nearly unstrained due to the fairly good lattice match. On the contrary, the 50 nm FeSe film on MgO is not fully relaxed and under tensile strain. The tensile strain of the 50 nm FeSe film on STO is somewhat larger.

Figure 2 shows the resistance as a function of temperature for the FeSe films on MgO, STO, and LAO substrates. An abrupt decrease of the resistance at low temperature is observed for all thick (100 nm and 200 nm)

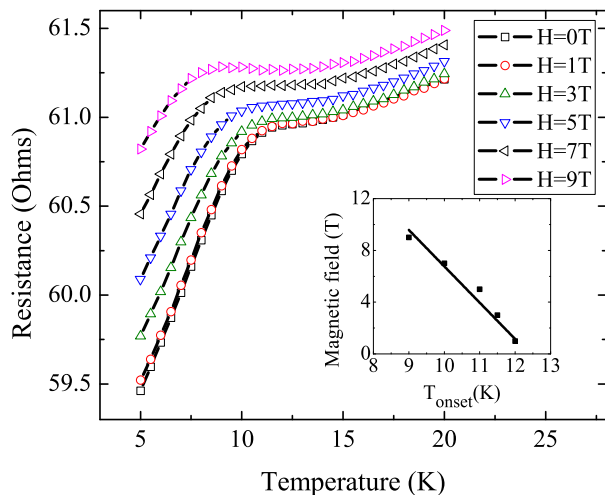


FIG. 3: (color online) Resistance as a function of temperature with various external magnetic fields for 50 nm FeSe film on LAO. The insert shows the external magnetic field as a function of the superconducting onset temperature.

FeSe films, but only for one thin (50 nm) film, the film on LAO. We attribute this drop to the onset of superconductivity. This is because the film T_{onset} values are approximately 8 K, which coincide with the value for bulk polycrystalline FeSe [8]. Furthermore, T_{onset} exhibits a magnetic field dependence; when the magnetic field increases, T_{onset} decreases. Figure 3 shows the resistance as a function of temperature with various external magnetic fields for 50 nm FeSe film on LAO. The insert shows the external magnetic field as a function of the superconducting onset temperature. The values for T_{onset} are

chosen as the temperature where the resistance start to decrease abruptly. The linearly extrapolated y-intercept value is estimated to be 35 T, which is similar to the value for single crystal FeSe [17], but about twice that for powder samples [8].

The resistance measurements described above demonstrate that the unstrained FeSe films show bulk-like properties with a $T_{onset} \approx 8$ K. The 50 nm films on MgO and STO are under tensile strain with no superconducting transitions down to 5 K. The strained 50 nm FeSe films are grown under the same condition as the 200 nm FeSe films, and they are comparable in quality. The XRD patterns are as good as the other films, the resistance is similar to the other films, and most importantly, they are metallic down to 5K with no upturn due to charge localization. This implies that the superconductivity is not simply suppressed by having a poor quality film that lacks a current path of the proper phase. The tensile strain itself suppresses the superconductivity.

In summary, we grew 50 nm, 100 nm, and 200 nm tetragonal α -phase FeSe epitaxial films on various substrates by PLD. The structure of the FeSe films depends strongly on the growth conditions and the lattice mismatch with the substrates. All thick (100 nm and 200 nm) films, and all films on LAO are mostly unstrained, and behave like the bulk material. Thin (50 nm) FeSe films on MgO and STO are under tensile strain. Evidence of superconductivity has been observed in unstrained FeSe films, with T_{onset} close to that of bulk material. No sign of superconductivity has been observed in FeSe films under tensile strain down to 5 K. This implies that tensile strain suppresses superconductivity.

This work is supported by the US-DOE through contract # DE-FG02-00ER45801.

-
- [1] Y. Kamihara, T. Watanabe, M. Hirano, and H. Hosono, *J. Am. Chem. Soc.* **130**, 3296 (2008).
- [2] H. Takahashi, K. Igawa, K. Arii, Y. Kamihara, M. Hirano, and H. Hosono, *Nature* **453**, 376 (2008).
- [3] X. H. Chen, T. Wu, G. Wu, R. H. Liu, H. Chen, and D. F. Fang, *Nature* **453**, 761 (2008).
- [4] C. de la Cruz, Q. Huang, J. Lynn, J. Li, W. RatcliffII, J. L. Zarestky, H. A. Mook, G. F. Chen, J. L. Luo, N. L. Wang, et al., *Nature* **453**, 899 (2008).
- [5] J. G. Bednorz and K. A. Müller, *Z. Phys. B* **64**, 189 (1986).
- [6] M. Rotter, M. Tegel, and D. Johrendt, *Phys. Rev. Lett.* **101**, 107006 (2008).
- [7] M. J. Pitcher, D. R. Parker, P. Adamson, S. J. Herkelrath, A. T. Boothroyd, R. M. Ibberson, M. Brunelli, and S. J. Clarke, *Chemical Communications* **45**, 5918 (2008).
- [8] F.-C. Hsu, J.-Y. Luo, K.-W. Yeh, T.-K. Chen, T.-W. Huang, P. M. Wu, Y.-C. Lee, Y.-L. Huang, Y.-Y. Chu, D.-C. Yan, et al., *Proc. Natl. Acad. Sci. U.S.A.* **105**, 14262 (2008).
- [9] K. Terzieff, P. Komarek, *Monats. Chem.* **109**, 651 (1978).
- [10] W. Schuster, H. Mikler, and K. L. Komarek, *Monats. Chem.* **110**, 1153 (1979).
- [11] K.-W. Yeh, T.-W. Huang, Y.-L. Huang, T.-K. Chen, F.-C. Hsu, P. M. Wu, Y.-C. Lee, Y.-Y. Chu, C.-L. Chen, J.-Y. Luo, et al., *Europhys. Lett.* **84**, 37002 (2008).
- [12] Y. Mizuguchi, F. Tomioka, S. Tsuda, T. Yamaguchi, and Y. Takano, *Appl. Phys. Lett.* **93**, 152505 (2008).
- [13] S. Margadonna, Y. Takabayashi, Y. Ohishi, Y. Mizuguchi, Y. Takano, T. Kagayama, T. Nakagawa, M. Takata, and K. Prassides (2009), arXiv: 0903.2204.
- [14] G. Garbarino, A. Sow, P. Lejay, A. Sulpice, P. Toulemonde, W. Crichton, M. Mezouar, and M. Nunez-Regueiro (2009), arXiv: 0903.3888.
- [15] J. N. Millican, D. Phelan, E. L. Thomas, J. B. Leao, and E. Carpenter, *Solid State Commun.* **10**, 1016 (2009).
- [16] A. Matthews, J.W. Blakeslee, *J. Cryst. Growth* **27**, 118 (1974).
- [17] U. Patel, J. Hua, S. H. Yu, S. Avci, Z. L. Xiao, H. Claus, J. Schlueter, V. V. Vlasko-Vlasov, U. Welp, and W. K. Kwok, *Appl. Phys. Lett.* **94**, 082508 (2009).